III. PLASMA HEATING AND CONTAINMENT

Warren D. Rayle, John J. Reinmann, J. Reece Roth,
and Donald R. Sigman

One of the most important goals of our work on plasma heating and confinement is the possibility of controlled thermonuclear fusion for space power and propulsion. As pointed out in the INTRODUCTION, the thermonuclear rocket is potentially the best propulsion system yet envisioned for missions with large payloads. Although this discussion will be oriented toward fusion, we also have a broader objective which is to acquiare knowledge and to obtain a better understanding of plasma processes. Such knowledge and understanding are useful for other potential applications of plasma technology.

Controlled fusion research has been conducted by many talented scientists for nearly two decades. No one can predict just when fusion will become a reality. In the meantime, we need to keep abreast of new results and knowledge in this important sector of plasma physics. Active work in the plasma heating and confinement fields not only serves this purpose but also permits us to make significant contributions which aid both the study of fusion and other aspects of plasma technology in which NASA has a vital interest.

After presenting a brief review of some of the basic factors of interest to controlled fusion, a sample of the NASA Lewis work in the plasma heating and confinement areas will be presented. Two plasma heating studies will be covered in some detail. Work related to the understanding of plasma losses from confinement will be briefly touched upon.

FUSION CONSIDERATIONS

A good estimate of the required operating parameters of a fusion reactor may be obtained by performing energy-balance calculations on the overall power plant. The light elements of interest for fusion reactors are deuterium, tritium, and helium-3. The deuterium-tritium fuel mixture, which releases most of its energy in the form of high-energy neutrons, is considered for ground power applications. The deuterium - helium-3 mixture releases most of its energy to charged particles,

and it will be used for space propulsion or for direct conversion of charged-particle energy into electrical power.

Some of the required parameters for deuterium - tritium or deuterium - helium-3 reactors are shown in the following table:

Temperature, K	10^8 to 10^9
Confinement time, sec	0.1 to 1.0
Density, particle/m^3	10^{20} to 10^{22}
Magnetic field, T	5 to 10

If positively charged ions are to undergo a fusion collision, then as they approach each other, their kinetic energies must be high enough to overcome the electrostatic repulsion. This requires plasmas with extremely high ion temperatures on the order of 10^8 to 10^9 degrees.

The probability that a particle will undergo a fusion event is proportional to the amount of time the particle remains in the reactor (confinement time). Feasibility studies indicate that confinement times on the order of 0.1 to 1 second are required.

The fusion power density is porportional to the square of the plasma number density. For the power levels of interest, number densities on the order of 10^{20} to 10^{22} particles per cubic meter are required.

In all proposed fusion reactor schemes, plasmas are confined with the aid of magnetic fields. The field strengths required are on the order of 5 to 10 teslas. To efficiently produce these high fields over the large reactor volumes, we would use superconducting coils.

The major obstacle in fusion research is inadequate confinement time. The longest confinement time in a thermalized, hot-ion plasma experiment is about 0.02 second, and most experiments give times on the order of a millisecond or less. Because of these rapid loss rates, it is difficult to produce a high-density, high-temperature plasma. Therefore, the major fusion research problems at present are (1) plasma confinement and (2) plasma production and heating.

Confinement studies are conducted in several different magnetic-field configurations. These magnetic geometries include both open-ended, and closed systems. Examples of these two systems are shown in figures III-1 and III-2. Figure III-1 is an example of an open-ended magnetic-mirror machine. Radial diffusion to the walls is reduced by the axial magnetic fields, while plasma end losses are reduced by increasing the field intensity at the ends. Some of the plasma approaching the ends gets reflected back towards the center of the machine. The higher field regions are therefore called magnetic mirrors.

A toroidal magnetic geometry (shown in fig. III-2) was devised to eliminate end losses of mirror systems. Plasma circulates around the major axis of the

torus and diffuses along the minor radius to the walls.

Until recently, the experimental loss rates in both of these geometries exceeded the classical, or collisional loss rates. These anomalously high losses are generally attributed to plasma instabilities. A plasma can become unstable in many ways, including both macroscopic and microscopic instabilities. In a macroscopic instability there is gross motion of the plasma to the wall. Gross motions can be controlled by magnetic wells and by magnetic shear configurations, to be discussed later. The microscopic instabilities are more akin to fluid dynamic turbulence. The result of these instabilities is increased diffusion to the wall. They may be caused by density and temperature gradients in the plasma or by non-Maxwellian velocity distributions of the ions or electrons.

All these instabilities derive from the fact that the plasma is not in a true state of thermodynamic equilibrium, If the plasma relaxes to the equibrium state, it can release free energy that can drive the instabilities. To avoid this, we must either eliminate the nonequilibrium condition or prevent the plasma from relaxing to the equilibrium state.

The magnetic-well concept is a means of preventing the plasma from relaxing to the equilibrium state. This concept is illustrated in figure III-3. The circles represent surfaces of constant magnetic-field intensity. The center of the circles is the minimum magnetic-field intensity point. The intensity increases away from the center. The plasma is placed in the center of the magnetic well. Since the plasma is dimagnetic, if it tries to move outward into the higher field intensity region, it will be pushed back toward the center. These surfaces of constant magnetic-field intensity should not be confused with the magnetic-field lines. The field lines actually intersect these surfaces.

An example of an open-ended magnetic-well configuration is shown in figure III-4. To produce the magnetic well, so-called quadrupole fields are superposed on the simple magnetic mirror. The quadrupole field consists of four linear conductors alined parallel to the axis of the mirror field. The current in adjacent bars runs in opposite directions and produces the magnetic-field pattern shown in the upper right-hand corner of the figure. The result of superposing the two fields is shown at the bottom. The magnetic well is located in the central region. Magnetic wells have proved completely effective in eliminating macroscopic instabilities in open-ended systems.

Although it is not obvious from figure III-4, the magnetic-field lines must bulge toward the center of the plasma in a magnetic well. When field lines close on themselves, as in a torus, it is not possible to have the field lines bulge toward the plasma everywhere. Therefore, a true magnetic well is not possible in the toroidal geometry. However, theory shows that the macroscopic instabilities may be stabi-

lized in toroids by using average magnetic wells. An example of a toroidal average magnetic well is shown in figure III-5. Four current-carrying conductors are immersed in the plasma. The current flows in the same direction in all four bars. The magnetic-field pattern is shown in the inset. In the central region, the field lines bulge toward the plasma, but in the region outside the bars, the field lines bulge away from the plasma. These so-called toroidal multipoles are valuable for testing theory, and for gaining insight into the mechanisms of diffusion. But since the conductors are immersed in the plasma, they could not be used in a fusion reactor. The conductors would be burned up by the hot plasma.

The other way to control macroscopic instabilities in a torus is by application of magnetic shear. A toroidal machine with magnetic shear would have field lines as shown in figure III-6. The field lines spiral around the minor axis, and the amount of twist of the spiral varies along the minor radius.

Toroidal shear fields are produced by the usual toroidal windings plus another set of current-carrying conductors. These additional conductors can either be placed external to the plasma or be immersed in the plasma. Since a fusion plasma has very high electrical conductivity, the plasma can act as a current-carrying conductor. By transformer action a current can be induced to flow in the plasma along the minor axis to provide the shear field. The experiment that has produced the best combination of confinement time, ion temperature, and density was conducted in the Tokamak T-3, a toroidal machine with magnetic shear. This Russian machine has received a great deal of publicity lately. In this experiment the magnetic shear is produced by inducing a current to flow in the plasma along the minor axis of the torus.

Let us now consider methods to control microscopic instabilities. Because of the relatively simple geometry of the open-ended systems, the theoretical understanding of microscopic instabilities in such systems is fairly complete. The theory also suggests ways of eliminating most of the instabilities. This usually requires a more randomized ion velocity distribution than can be produced experimentally at this time. Unfortunately, even if the instabilities are controlled, and the losses are caused only by classical diffusion, the energy balance is marginal. Some way is needed to further reduce the end losses below the classical values to make a feasible reactor. There are several methods under study to reduce mirror end losses. The feasibility of open-ended machines will probably rest on the success of these schemes.

In toroidal systems, there are some indications that both macroscopic and microscopic instabilities occur. Unfortunately, the toroidal geometry is so complicated that the theory of microscopic instabilities is far from complete, and there are fewer theoretical guidelines for their control. Until about 1965, experimental confinement

times in toroidal machines were in approximate agreement with the so-called Bohm diffusion equation. The confinement time for Bohm diffusion is directly proportional to the magnetic field and inversely proportional to the electron temperature:

$$\tau_{\text{Bohm}} \propto \frac{B}{T_e}$$

This is an empirical relation that Bohm found to hold in experiments conducted on ion sources in magnetic fields. Bohm offered no theoretical derivation of the relation, but the same functional form of the variables can be derived by the use of a dimensional argument.

In contrast, the confinement time for classical or collisional diffusion is proportional to the square of the magnetic field and to the square root of the electron temperature:

$$\tau_{\text{classical}} \propto \frac{B^2 T_e^{1/2}}{n}$$

For typical reactor design conditions the classical confinement time is several orders of magnitude larger than the Bohm confinement time.

Fortunately, in a toroidal machine classical confinement times are not required. The actual confinement time must be about 100 to 1000 times that of Bohm. This is one clear advantage that the toroidal machine has over the open-ended system. As previously noted, in a feasible open-ended system, the end losses will probably have to be less than the classical losses.

After 1965, experimental confinement times in toroidal systems continued to increase up to about 100 Bohm times. Very recently, it was announced that 300 Bohm times were achieved in a toroidal multipole experiment. Thus, prospects for toroidal machines look good.

It is worth pointing out that relatively long confinement times are not the only encouraging feature of the recent toroidal experiments. In his recent talk at the Bucharest meeting, Galeev reported that radial diffusion in the Tokomak could be explained entirely by binary collisions, without having to invoke collective effects or some instability related diffusion process. The loss rate is higher than classical diffusion because the average random-walk step size in the Tokomak is the average separation between drift surfaces before and after a binary collision. These drift surfaces are separated by a distance greater than the gyroradius, which is the step size for classical diffusion.

It would certainly simplify matters considerably if classical scattering ideas could explain the losses in the toroidal machines.

The present status of one aspect of fusion research can be summarized with the aid of the so-called Lawson diagram (see fig. III-7). This is a plot of ion temperature against the product of density and confinement time. In energy balance calculations, n and τ always appear as the product. A reactor will operate in the upper right-hand corner. The darker the shading, the better the chance for a workable reactor.

The 2X and Scylla machines are open-ended machines in the United States. The C-stellarator is a toroidal machine at the Princeton Plasma Physics Laboratory, and Tokamak is a Russian toroidal machine. The arrows lead to open circles which are the predicted operating points for new machines that are being built and that will be operational in a few years. If the scaling laws are correct for these machines, this would indeed be significant progress toward controlled fusion. Incidentally, the C-stellarator is now being converted into a Tokamak machine.

ION-CYCLOTRON RESONANCE HEATING

Theoretical Considerations

The problems of confinement and stability have received a great deal of attention, and progress is evident. Here at Lewis Research Center, we have devoted a greater fraction of our experimental effort to problems of plasma heating, particularly in the steady state. One such study involves the use of ion-cyclotron resonance heating. This is a process whereby energy is transferred to a plasma in the form of electromagnetic waves. Then, once in the plasma, the wave energy is converted to ion energy.

A plasma column such as shown in figure III-8 will support the propagation of electromagnetic waves. If a current carrying coil is wrapped around the plasma column and excited by a generator of frequency ω, energy can be transferred to a set of waves called natural modes that satisfy the boundary conditions of the plasma and can thus propagate along the column. The wavelengths of these modes are functions of the plasma parameters and the boundary conditions. For waves with a frequency approximately equal to the ion-cyclotron frequency, the wavelengths are strongly dependent on the magnetic field confining the plasma.

The concept of cyclotron heating requires that energy from a specially constructed radiofrequency coil be coupled into these waves in the plasma at frequencies slightly below the ion-cyclotron frequency. Because the current directions in adja-

cent coil sections are opposite, this specially designed coil (called a Stix coil after its inventor) produces fields which vary sinusoidally in the axial direction. The coil can thus be said to have a wavelength λ_0 associated with it which equals the distance between corresponding points on the first and third sections. With a coil like this, it is then possible to couple significant amounts of energy to a natural mode of the plasma when the wavelength of the coil is the same as that of the natural mode. Thus, in a wavelength sense, there exists a resonance coupling. The wavelength of a natural mode is usually made to match that of the coil by varying the magnetic field.

Recently, many calculations of the power that could be transferred to these plasma waves by a Stix coil have been made. A parametric study has included the effects of magnetic field, density, density gradients, temperature, and collisions as well as geometric effects such as plasma column radius and radiofrequency coil dimensions. The results of some of our calculations are shown in figure III-9 as curves of power transferred to the plasma against magnetic field with ion temperature as a parameter. For fields such that the wave frequency equals the ion-cyclotron frequency, the efficiency of coupling is low. But, as the magnetic field is increased, the wavelengths of the most fundamental natural modes become closer to that of the Stix coil. Finally the wavelength resonance is achieved, and there is a maximum in the coupling. Under proper conditions the efficiency of coupling can be 80 percent.

One of the more interesting parameters studied with regard to power transfer is that of ion temperature. We found that, as the ion temperature increases, the maximum power transfer to the plasma decreases. This is also shown in figure III-9. In this figure the Stix coil wavelength was 41 centimeters and the electron density 2×10^{18} particles per cubic meter. The reduction in coupling with increased temperature is more severe for shorter Stix coil wavelength and/or lower electron density. Efficient coupling of energy to waves must be done in a part of the plasma where the ion temperature is not too high.

Once energy is coupled to the waves, they propagate along the plasma column out each end of the Stix coil. At this point the wave characteristics are studied to make sure the Stix coil has generated the wave with the characteristics desired for the next phase of the heating scheme, that of damping of the wave and conversion of the wave energy into ion energy. The waves will be damped by a process called ion-cyclotron damping if the wave propagates (as shown in fig. III-10) into a region where the confining field as a function of axial position has been lowered to the point where the ion-cyclotron frequency equals the wave frequency. In the region where the field has started to decrease, the wavelength will start to shorten, and the wave amplitude will increase in a manner similar to that of a water wave approaching a

beach. This region is therefore referred to as a "magnetic beach."

When the ion-cyclotron frequency becomes sufficiently close to the wave frequency, there will be many particles that feel the fields of the wave at exactly the cyclotron frequency and are thus heated. What is accomplished here is a heating of ions by a radiofrequency field whose effective (or Doppler shifted) frequency is the ion-cyclotron frequency.

This may appear to many as a rather cumbersome way to heat a plasma. First a plasma wave is generated; then the wave is used to heat ions. One would naturally prefer a more direct approach. Why not just wrap a simple solenoid around a plasma column and heat ions inside the coil by driving it at the ion gyrofrequency? This approach has been tried, but it was discovered that a space charge builds up in the plasma producing electric fields in opposition to those applied (i.e., there was a shielding of the plasma from the applied external field). Energy is transferred much more efficiently to the plasma in the wave generating scheme.

Experimental Work

Figure III-11 is a schematic of the steady-state ion-cyclotron resonance apparatus now being used at Lewis. There is a plasma column immersed in a magnetic field (maximum value, 1 tesla). The Stix coil (wavelength, 41 cm) is located in the center, and is supplied by a radiofrequency generator of 6.5 megahertz. The magnetic beach where the waves are damped is placed just inside the mirror. The region between the coil and the beach is where various probes are placed to measure the properties of the wave being propagated.

Figure III-12 shows a plot of measured power transfer to the plasma from the Stix coil against the applied direct-current magnetic field. There is a maximum in the coupling at a point very close to that predicted by the theory. Although it is difficult to know precisely all the plasma parameter values necessary to calculate the magnitude of the coupling, a "best guess" set of values may be used to predict the magnitude to within 20 percent.

We now look at some data taken in the region of propagation immediately outside the Stix coil. The ion-cyclotron wave has a time varying component of magnetic field in the axial direction, and the amplitude and phase of this field can be measured by a probe. The output of this probe is viewed as a sinusoidal signal on an oscilloscope where the amplitude is proportional to the strength of the wave and the phase is determined relative to the radiofrequency voltage on the Stix coil. Figure III-13 is a plot of the measured phase of the wave against the axial position of the probe for two different values of magnetic field. The distance over which a

phase change of 2π occurs equals the wavelength of the wave. Theory tells us that the closer the wave frequency is to the ion-cyclotron frequency, the shorter the wavelength (i.e., the steeper the slope of the curve). This is exactly what you see presented here with the wave frequency being closer to the cyclotron frequency for the curve on the left.

Now, let us move on to look at some data taken in the vicinity of the magnetic beach. Theoretically the amplitude of the axial magnetic field of the wave should increase as the magnetic field decreases, thus making the ion-cyclotron frequency approach the wave frequency. However, when the cyclotron frequency gets sufficiently close to the wave frequency, ion-cyclotron damping becomes strong, the wave amplitude decreases rapidly, and ions are heated. Figure III-14 shows measured wave amplitude plotted as a function of axial position. The wave is propagating to the right, and the magnetic field is decreasing to the right. The point labeled magnetic beach region is where the wave and cyclotron frequencies are equal. The amplitude initially increases and subsequently damps. The actual rate of damping and the point at which damping begins depends on the axial temperature of the plasma.

The ion motion perpendicular to the magnetic field produces a reduction in the direct-current magnetic field (i.e., a diamagnetism). By measuring this reduction in direct-current field, it is then possible to determine the temperature to show that we are truly heating the plasma with the ion-cyclotron wave. To measure the change, a diamagnetic loop is used. The change in magnetic flux is measured through this loop as the plasma is extinguished. Figure III-15 gives temperature (derived from diamagnetic loop measurements) as a function of axial position, and it clearly shows that in the vicinity of the magnetic beach the temperature is much higher than elsewhere, reaching a value greater than 500 electron volts at the center of the beach. The electron density of the plasma was about 2×10^{18} particles per cubic meter. In pulsed experiments at the Princeton Plasma Physics Laboratory ion-cyclotron heating has been used to heat plasmas in magnetic beaches to several kilovolts.

To summarize, it appears that ion-cyclotron damping is an efficient and effective way to heat plasma ions in plasmas contained in the simple magnetic configurations discussed. The question does remain, however, as to whether cyclotron heating will be effective in more complex confining fields devised for the purpose of making the plasma more stable. And whether this process proves usable on the ultimate fusion machines, either alone or in conjunction with other heating methods, it has already proven its value in producing hot, dense plasmas for fusion research. In our future plans, a major objective is to apply ion-cyclotron res-

onance heating (ICRH) to open-ended magnetic wells. The purpose of these tests is to experimentally study the generation, propagation, and damping of waves in the more complex magnetic fields of these wells.

Initial work on the well will be conducted on the present apparatus as shown on figure III-16. This experiment involves the conversion of one of our beaches into a shallow magnetic well by wrapping quadrupole windings around the test section. A later experimental study is planned for a superconducting magnetic mirror apparatus now under construction which will have the capability of producing magnetic fields up to 8 teslas.

One possible scheme for applying IRCH to an open-ended magnetic well is shown on figure III-17. Ion-cyclotron waves would be generated at the two ends of the system (in the mirrors) and propagate towards the center where they give up their energy to ions in the magnetic wells. This may have the added benefit of testing a scheme to reduce end losses in open-ended systems. Experiments at Princeton Plasma Physics Laboratory indicate that ions are accelerated away from the Stix coil. It may be possible to use this acceleration effect to keep particles from escaping out the ends of the magnetic well. As mentioned earlier, some method to reduce end losses is crucial to the feasibility of open-ended reactors.

MODIFIED PENNING DISCHARGE

A second type of plasma heating process being studied here involves the use of high-voltage direct-current power in what is called a "modified Penning discharge." These two heating studies represent an interesting contrast in approaches. In the ion-cyclotron heating work, you may recall, we started with a theoretical concept and attempted to verify it experimentally and to refine and improve it. In the high-voltage direct-current heating study, we started with an experimentally observed phenomenon and attempted to construct a theoretical model and to improve the process experimentally.

Initial Observations of Ion Heating

A magnetic mirror machine is created by two superconducting coils located in a 1-meter-diameter vacuum tank. (Figs. III-18 and III-19 are schematics of the experiment configuration.) It is possible to produce a maximum magnetic field up to 2.0 teslas at the coils. The anode ring has a high positive dc potential of up to several tens of kilovolts. Neutral molecules within the containment volume are ionized by trapped electrons. The ions produced are heated by fluctuating electric fields

and are eventually lost out of the mirrors. A photograph of the plasma is shown in figure III-20. The shape of the plasma conforms to that of the magnetic field. The vertical element in the middle is the anode ring, which is maintained at a high positive potential.

The energy of the ions escaping through one of the magnetic mirrors was measured with a retarding potential-energy analyzer. The curve of figure III-21 represents the flux of ions whose axial energy exceeds the value shown on the abscissa. Also shown is the best-fitting integrated Maxwellian distribution curve. This curve has several interesting features not anticipated at the outset of the experiment. The first is that the velocity distribution is Maxwellian along a radius in velocity space, even in the high-energy tail. It was surprising to find that the particles were thermalized in the relatively short time (typically 25 μsec) and that they were confined between the mirrors. The second interesting feature was the very high ion kinetic temperatures observed (710 eV, in the case shown). These high ion temperatures were accompanied by low electron temperatures (no more than about 200 eV). These features are very desirable in fusion applications, since one normally prefers to dump the power supply energy into the ions rather than the electrons. The Maxwellianization of the ion velocity distribution is desirable, since the plasma will contain one less reservoir of free energy to drive macroscopic and microscopic instabilities.

These high ion temperatures were investigated further, with the results shown in figure III-22. The ion kinetic temperature is shown plotted as a function of direct-current anode voltage for four background pressures of deuterium gas. The kinetic temperature is approximately linearly proportional to the anode voltage up to the limit of the power supply used. This suggests that ions of any desired energy can be produced by going to a sufficiently high anode voltage. The only other steady-state heating system to produce such high ion temperatures is the Burnout-V device at Oak Ridge National Laboratory. There the ions are accompanied by very hot electrons, up to several hundred keV in energy, so a different heating process is probably operating in that case.

Continuity-Equation Oscillation

The interesting results from this modified Penning discharge demanded an understanding of the physical phenomena responsible for them. A floating Langmuir probe was inserted into the plasma to study the spectrum of the electrostatic potential fluctuations. The output of this probe was connected to a spectrum analyzer, with the results shown in figure III-23. The peak at zero frequency is an internally generated marker. This spectrum reveals a fundamental at about 6800 hertz, sev-

eral harmonics, and a continuous spectrum that can be followed out to 2 megahertz.

It is tempting to make the analogy with conventional hydrodynamics and explain the high ion kinetic temperatures as a consequence of energy being dumped from the power supply into the plasma at the fundamental frequency, followed by a cascading up in frequency and down in scale size until it is dissipated in thermal energy of the ions.

The characteristics of this turbulence spectrum were studied to see whether this might explain the high ion energies. The identification of the fundamental frequency immediately presented a problem. Its low frequency (6800 Hz in the example shown) in a mirror field whose maximum value was typically 1 tesla was much too low to be associated with the plasma frequency or the ion or electron gyrofrequencies. It was also too low by orders of magnitude to be plausibly connected with $E \times B$ or grad-B drifts. Parametric variation of the plasma properties showed that the frequency of this oscillation depended on both the electron and neutral number densities, but not on the magnetic field.

The retarding potential energy analyzer was used to measure the efflux of ions as a function of time. Results are shown in figure III-24. The zero level is the baseline between pulses. The charged-particle efflux displays pulsar-like sharp, narrow peaks between broad, flat minima. For different plasma conditions, these pulses display fine structure, periodic interpulses and other interesting detailed features. The particle efflux, the light output, and the electrostatic fluctuations were in phase at the same frequency. The light output was monitored at two axial and azimuthal stations with a pair of photomultipliers, and showed that the plasma was oscillating in unison with a single phase and frequency.

These characteristics suggested that the oscillation in question is a new phenomenon, and this subsequently proved to be the case. This oscillation was labeled the continuity-equation oscillation, because it arises as a consequence of periodic solutions to the coupled pair of continuity equations for neutrals and charged particles in a slightly ionized gas. The frequency is porportional to the square root of the product of electron and neutral number densities, and is independent of magnetic field. An exact solution to this pair of equations is shown in figure III-25. The ordinate is relative electron number density; the abscissa is time. There are four values of the relative peak-to-peak amplitude η. At high peak-to-peak amplitudes, the solutions have the characteristic waveform we saw in the particle efflux - sharp, narrow peaks between broad, flat minima.

The oscillation frequency was systematically studied as a function of the electron and neutral number densities. Figure III-26 shows the results. The observed frequency is plotted as a function of the product of relative electron and neutral

number density. The square root dependence predicted theoretically holds over a range of 5 orders of magnitude in the density product.

The oscillation arises from an effect usually ignored in elementary kinetic theory arguments: The transit time delays that result when particles move along their mean free path to the point of interest. The effect is most apparent in apparatus like this one, in which the mean free paths are relatively long. These time delays introduce a lag between the particle production and loss processes in the plasma, and this, in turn, causes a relaxation oscillation in the neutral and charged-particle number densities.

That's the interpretation of the physical phenomena as they occur in this experiment. It seems possible, though, to describe the class of oscillations in more general terms. Whenever the production rate of each species depends on factors including the instantaneous populations of both species, one may look for oscillatory solutions. These oscillations can occur in other contexts. Similar pairs of equations have been used to describe ecological systems in which there occur periodically fluctuating populations of predator and prey. They have also been used to describe certain oscillatory chemical reactions.

In this modified Penning discharge, the characteristics of the oscillation depend solely on the parameters appearing in the two continuity equations. The equations representing conservation of momentum and energy must be satisfied, of course, but they play no role in the oscillation beyond determining the coefficients of the terms in the continuity equations.

Observations of Quasi-Linear Mode Coupling

With an explanation of the fundamental oscillation frequency, attention was then turned to understanding other aspects of the ion heating process. The ion heating process was studied with the apparatus shown in figure III-27. A powerful alternating-current amplifier was connected to the anode ring in parallel with the high-voltage, direct-current supply normally used. The effect of a sinusoidal excitation imposed on the anode ring on the spectrum of electrostatic potential fluctuations was measured with the capacitive probe shown. The resulting spectra for two background pressures are shown in figures III-28 and III-29. The frequency range is from zero to 100 kilohertz. The externally excited frequency is on the left, followed by several of its harmonics. At higher frequencies, one can see the continuity-equation frequency, its harmonics, and sideband modulations at the imposed frequency. It seems a clear illustration of quasi-linear mode coupling in the plasma, and is particularly interesting in view of the very low frequencies involved

and the presence in the background of a continuous, fully developed, nonlinear turbulent spectrum.

The following table summarizes the best temperatures, densities, and confinement times simultaneously observed in this experiment thus far:

Ion kinetic temperature, T_i, keV	5
Electron kinetic temperature, T_e, eV	200
Plasma number density, n_e, particle/m^3	2×10^{16}
Ion confinement time, μsec	27

The ion temperatures listed are gratifying, but the densities and confinement times are quite low. These are now limited by the rapid loss of ions out the mirrors. Confinement time and density can be improved with a closed configuration such as shown in figure III-30 - a bumpy torus. This consists of 12 magnetic mirrors end-to-end in a toroidal array. Such a superconducting magnet facility is presently under consideration for future use in this experiment. The modified Penning discharge scheme will be applied to this configuration. It is one of the few steady-state plasma injection and heating schemes capable of being applied to a toroidal geometry. A reasonable goal for the bumpy torus would be an increase of a factor of 10 in confinement time and number density.

STUDIES RELATED TO CONFINEMENT

Random-Walk Approximation

Two studies related to confinement are underway at Lewis. One of these, an analytical approach, uses a computer to simulate the plasma behavior. Gerald Englert has been developing a technique which may permit the approximate solution of plasma problems over a wide range of conditions. He calls this technique "random-walk approximation." To date he has applied it to the problem of particle diffusion in velocity space in a magnetic-mirror configuration. The basic idea is this: Let the particle's velocity be represented by a magnitude V and an angle to the magnetic field θ. The changes in velocity resulting from collisions with other particles can be represented as probabilities. There is a certain probability that the velocity will change by an increment in V and in θ.

Given expressions for these probabilities, the computer can "walk" the particles over a two-dimensional grid in velocity space. By using iterations, and reasonably large steps, an equilibrium distribution of particles can be found without undue computer time. The probabilities that bias the random walk are obtained by

comparing the random-walk with the Fokker-Planck equation, and assuming the coefficients of like terms to be the same. The procedure is not the same as the Monte Carlo method. Monte Carlo would select a step of variable length and direction, based on the physics of binary encounters. The random-walk method takes large steps, in effect averaging over a large number of binary encounters, thereby reducing computer time.

Figure III-31 shows the equilibrium solution for one test case. The distribution in velocity magnitude is plotted; that is, the relative number of particles possessing any particular value of V. The case chosen was one for which an analytical approximation was available (shown by the curve). Note that the random-walk values exhibit approximately the same shape as the analytical result, and that the two values of mirror ratio show little effect.

Another question of great interest is the rate at which particles escape from the system. (They migrate into the loss cone.) Figure III-32 shows the random-walk loss rate plotted against the reciprocal of the logarithm of the mirror ratio. A good, linear fit is evident. This agrees with the functional relation predicted by some of the analytical approximations for this case.

In principle, the random-walk method could be used for more complex cases. Englert has started looking at cases involving physical space gradients. The big question to be answered is where do we get the values of the random-walk biases for more complex cases? Possibly, experiment might provide them.

Plasma Turbulence

The phenomenon of anomalous diffusion has often been associated with fluctuations in the plasma, although the nature of the connection in many real plasmas has yet to be rigorously established. As yet, the nature of the fluctuations to be expected in any given plasma cannot be predicted. First, we need a better understanding of the fluctuations as they actually occur. What is the spectrum? What is the source of energy? How are the various frequencies related? Is the fluctuation a purely random process or does it possess a coherence in space or time? For that matter, which plasma parameters are doing the fluctuating: density, temperature, or potential?

John Serafini, studying this problem has given us some answers. In figure III-33 his experimental device is shown. This is a crossed field device: the electric field is axial, the magnetic field radial. Into the annular plasma volume probes of various sorts may be inserted to detect the locally fluctuating quantities.

Using Langmuir probes, he obtains turbulence spectra such as are shown in figure III-34. Notice that for the three operating conditions, generally similar spectra occur. A peak appears at a relatively low frequency followed by a rather smooth decline at higher frequencies. For these measurements, the fluctuating quantity is the plasma density - a conclusion based on the behavior of the probe as the bias was varied. A detailed study of the spatial correlation of the various parts of the spectrum shows that the peak represents a coherent plasma oscillation - a helical mode. The higher frequencies are noncoherent, with no measurable propagation lag. There is, then, the superposition of two basically different kinds of fluctuations. The relation of these two types of fluctuations may be seen from figure III-34. Notice that the ordinate is a logarithmic scale, so that the actual amplitude varies quite substantially along the three curves. The increasing strength of the coherent oscillation - the peak of the curve - is accomplished by a rising level of signal strength even at the very high frequencies. Such a concurrent variation suggests that the energy in the high-frequency part of the spectrum derives from the coherent oscillation. Many means may be proposed to account for the coupling or energy transfer within the spectrum. The important implication is that the existance of a single mode of plasma oscillation may induce quasi-random or turbulent fluctuations over a wide frequency range. The data do not provide conclusive proof of this relation. However, the concept of energy being supplied via a coherent plasma oscillation, and thence to the turbulent spectrum at higher frequencies is intuitively appealing and consistent with the available data.

It is particularly important to determine experimentally the connection between turbulence or fluctuations of various kinds and the actual diffusion of the plasma particles across the magnetic field. A new device with parallel magnetic and electric fields is being constructed to permit such measurements.

In summary, we have discussed some of the basics of the fusion research field and dwelt on the two steady-state heating processes being studied here at Lewis. In addition, we have touched briefly on work related to plasma confinement and losses from confinement. The purpose of this discussion has not been to present a comprehensive or even a well-balanced picture of our work in these fields. Rather we have tried to convey our viewpoints and objectives, and a summary of the results we have obtained in our studies.

BIBLIOGRAPHY

This bibliography comprises publications authored by the members of the NASA Lewis Research Center Staff.

Englert, Gerald W.: Towards Thermonuclear Rocket Propulsion. New Scientist, vol. 16, Oct. 4, 1962, pp. 16-18.

Englert, Gerald W.: Study of Thermonuclear Propulsion Using Superconducting Magnets. Third Symposium on Engineering Aspects of Magnetohydrodynamics. Norman W. Mather and George W. Sutton, eds., Gordon and Breach Science Publ., 1964, pp. 645-671.

Englert, Gerald W.: High-Energy Ion Beams Used to Accelerate Hydrogen Propellant Along Magnetic Tube of Flux. NASA TN D-3656, 1966.

Flax, Lawrence: Theoretical Investigation of Ultrasonic Attenuation for Free Electrons in the Presence of a Magnetic Field. NASA TN D-3723, 1966.

Flax, Lawrence; and Simmons, Joseph H.: Magnetic Field Outside Perfect Rectangular Conductors. NASA TN D-3572, 1966.

Flax, L.; and Trivisonno, J.: Oscillatory Magnetoacoustic Attenuation. Phys. Letters, vol. 22, no. 5, Sept. 15, 1966, pp. 569-570.

Hettel, Henry J.; Krawec, Roman; Prok, George M.; and Swett, Clyde C.: Enhancement of Ion Cyclotron Waves in Hydrogen Helium Mixtures. NASA TN D-4271, 1968.

Howes, Walton L.: Effect of Initial Velocity on One-Dimensional, Ambipolar, Space-Charge Currents. NASA TN D-2425, 1964.

Krawec, Roman: An Instrument for Electronic Differentiation of Current-Voltage Characteristics. NASA TN D-2161, 1964.

Krawec, Roman: Steady-State Composition of a Low-Density Nonequilibrium Hydrogen Plasma. NASA TN D-3457, 1966.

Krawec, Roman: Radial Density and Temperature Profiles at the Ion Cyclotron Wave Resonance Point. AIAA J., vol. 4, no. 12, Dec. 1966, pp. 2166-2170.

Krawec, Roman: Electronic Analog for Performing Abel Inversion. Rev. Sci. Instr., vol. 39, no. 3, Mar. 1968, pp. 402-404.

Krawec, Roman: General Operating Characteristics of a Backstreaming Direct-Current Plasma Generator. NASA TN D-4604, 1968.

Krawec, Roman; Prok, George M.; and Swett, Clyde C.: Evaluation of Two Direct-Current Methods of Plasma Production for Use in Magnetic Mirror Experiments. NASA TN D-2862, 1965.

Maslen, S. H.: Fusion for Space Propulsion. IRE Trans. on Mil. Elect., vol. MIL-3, no. 2, Apr. 1959, pp. 52-57.

Monnin, Carl F.; and Prok, George M.: Comparison of Gryzinski's and Born's Approximations for Inelastic Scattering in Atomic Hydrogen. NASA TN D-2903, 1965.

Monnin, Carl F.; and Prok, George M.: Energy Transfer and Ion Cost in a Hydrogen Plasma. NASA TN D-5319, 1969.

Monnin, Carl F.; and Reinmann, John J.: Stability of Two-Fluid Wheel Flows with an Imposed Uniform Axial Magnetic Field. NASA TN D-5372, 1969.

Prok, George M.: Two-Step Process to Increase Atomic Hydrogen Ion Production in Low-Pressure Radiofrequency Discharge. NASA TN D-2912, 1965.

Prok, George M.; and McLean, Clifford A.: Intensity and Intensitv Ratio of Principal Singlet and Triplet Lines of Molecular Hydrogen. NASA TN D-2522, 1964.

Prok, George M.; and Monnin, Carl F.: Energy Required for Proton Production by Electron Impact in Mixtures of Atomic and Molecular Hydrogen. Bull. Am. Phys. Soc., vol. 13, no. 2, Feb. 1968, p. 299.

Prok, George M.; Monnin, Carl F.; and Hettel, Henry J.: Estimation of Electron Impact Excitation Cross Sections of Molecular Hydrogen. NASA TN D-4004, 1967.

Prok, G. M.; Monnin, C. F.; and Hettel, H. J.: Molecular Hydrogen Inelastic Electron Impact Cross sections - A Semiclassical Method. J. Quant. Spectrosc. Radiat. Transfer, vol. 9, no. 3, Mar. 1969, pp. 361-369.

Reynolds, Thaine W.; and Richley, Edward A.: Propellant Condensation on Surfaces near an Electric Rocket Exhaust. Presented at Seventh Electric Propulsion Conference, Williamsburg, Va., March 3-5, 1969.

Roth, J. Reece: Nonadiabatic Particle Losses in Axisymmetric and Multipolar Magnetic Fields. NASA TN D-3164, 1965.

Roth, J. Reece: Modification of Penning Discharge Useful in Plasma Physics Experiments. Rev. Sci. Instr., vol. 37, no. 8, Aug. 1966, pp. 1100-1101.

Roth, J. Reece: Optimization of Adiabatic Magnetic Mirror Fields for Controlled Fusion Research. NASA TM X-1251, 1966.

Roth, J. Reece: New Mechanism for Low-Frequency Oscillations in Partially Ionized Gases. Phys. Fluids, vol. 10, no. 12, Dec. 1967, pp. 2712-2714.

Roth, J. Reece: Plasma Stability and the Bohr - van Leeuwen Theorem. NASA TN D-3880, 1967.

Roth, J. Reece: Possible Applications of the Continuity-Equation Plasma Oscillation to Pulsars and Other Periodic Astrophysical Phenomena. NASA TN D-5078, 1969.

Roth, J. Reece: Periodic Small-Amplitude Solutions to Volterra's Problem of Two Conflicting Populations and Their Application to the Plasma Continuity Equations. J. Math. Phys., vol. 10, no. 8, Aug. 1969, pp. 1412-1414.

Roth, J. Reece: A Theory of Moving Striations Based on the Continuity-Equation Plasma Oscillation. Presented at the 9th International Conference on Phenomena in Ionized Gases, Bucharest, Romania, Sept. 1-6, 1969.

Roth, J. Reece; Freeman, Donald C., Jr.; and Haid, David A.: Superconducting Magnet Facility for Plasma Physics Research. Rev. Sci. Instr., vol. 36, no. 10, Oct. 1965, pp. 1481-1485.

Serafini, John S.: Correlation Measurements of Plasma Fluctuations in a Hall-Current Accelerator. Bull. Am. Phys. Soc., vol. 13, no. 2, Feb. 1968, p. 278.

Serafini, John S.: Utility of Conventional Turbulence Experimental Methods in the Study of Plasma Fluctuations. Bull. Am. Phys. Soc., vol. 13, no. 5, May 1968, p. 824.

Sigman, Donald R.: Radiofrequency Power Transfer to Ion-Cyclotron Waves in a Collision-Free Magnetoplasma. NASA TN D-3361, 1966.

Sigman, Donald R.; Krawec, Roman; Hettel, Henry J.; and Swett, Clyde C.: Further Experiments on Ion-Cyclotron-Wave Generation in the RF Self-Sustained Mode. Bull. Am. Phys. Soc., vol. 13, no. 11, Nov. 1968, p. 1509.

Sigman, Donald R.; and Reinmann, John J.: Ion Cyclotron Wave Generation in Uniform and Nonuniform Plasma Including Electron Inertia Effects. NASA TN D-4058, 1967.

Sigman, Donald R.; and Reinmann, John J.: Power Transfer to Ion Cyclotron Waves in a Two Ion Species Plasma. NASA TM X-1481, 1967.

Sigman, Donald R.; and Reinmann, John J.: Power Coupling and Wave Fields of Ion-Cyclotron Waves in a Finite Length System. Presented at the 10th Annual Meeting of the American Physical Society, Miami Beach, Fla., Nov. 13-16, 1968.

Swett, Clyde C.: Experiments on Inductive and Capacitive Radio-Frequency Heating of a Hydrogen Plasma in a Magnetic Field. NASA TN D-2717, 1965.

Swett, Clyde C.: Effect of Magnetic Beach on RF Power Absorption in Ion Cyclotron Resonance. Bull. Am. Phys. Soc., vol. 11, no. 4, June 1966, p. 450.

Swett, Clyde C.; and Krawec, Roman: Preliminary Observations of RF Power Transfer to a Hydrogen Plasma at Frequencies Near the Ion Cyclotron Frequency. Third Symposium on Engineering Aspects of Magnetohydrodynamics. Norman W. Mather and George W. Sutton, eds., Gordon and Breach Science Publ., 1964, pp. 599-614.

Swett, Clyde C.; and Krawec, Roman: Experiments on Ion-Cyclotron Wave Generation, Using an Electrostatically Shielded RF Coil. Bull. Am. Phys. Soc., vol. 10, no. 4, 1965, p. 509.

Swett, Clyde C.; and Krawec, Roman: Operation of an Ion-Cyclotron-Wave-Generation Apparatus in a RF Self-Sustained Mode. Bull. Am. Phys. Soc., vol. 13, no. 2, Feb. 1968, p. 278.

Woollett, Richard R.: Electromagnetic Wave Propagation in a Cold, Collisionless Atomic Hydrogen Plasma. NASA TN D-2071, 1964.

Woollett, Richard R.: Frequency Ranges for Existence of Waves in a Cold, Collisionless Hydrogen Plasma. NASA TN D-2273, 1964.

Woollett, Richard R.: Energy Addition to an Atomic Hydrogen Plasma at Off-Resonant Conditions. NASA TN D-2982, 1965.

Woollett, Richard R.: Error in Induced Electric Field Modes Under Stix Coil Resulting from Assumption of Orthogonality of Natural Plasma Modes. NASA TN D-3255, 1966.

Woollett, Richard R.: Magnitude of Nonlinearities in Collisionless Magnetoplasma Waves. NASA TN D-3778, 1967.

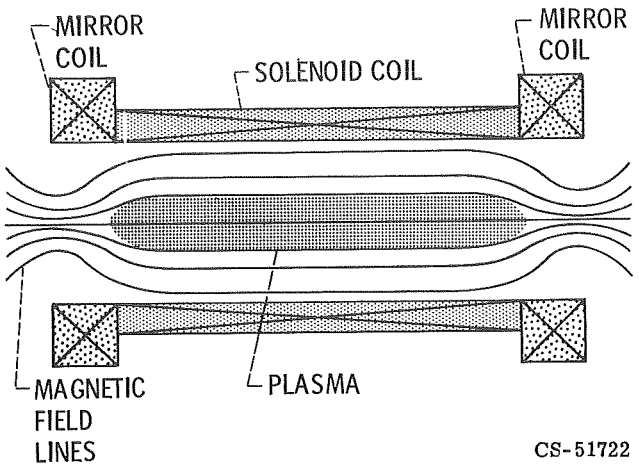

Figure III-1. - Plasma confined in magnetic mirror system.

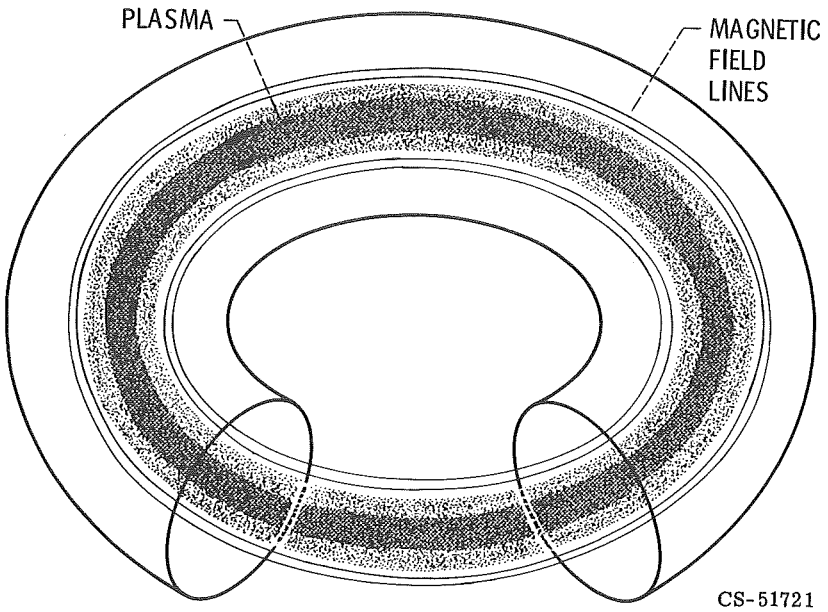

Figure III-2. - Plasma confined in torus.

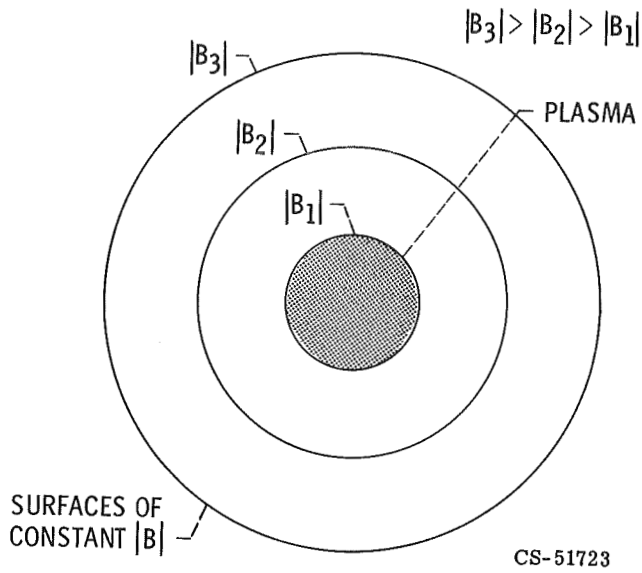

Figure III-3. - Magnetic well.

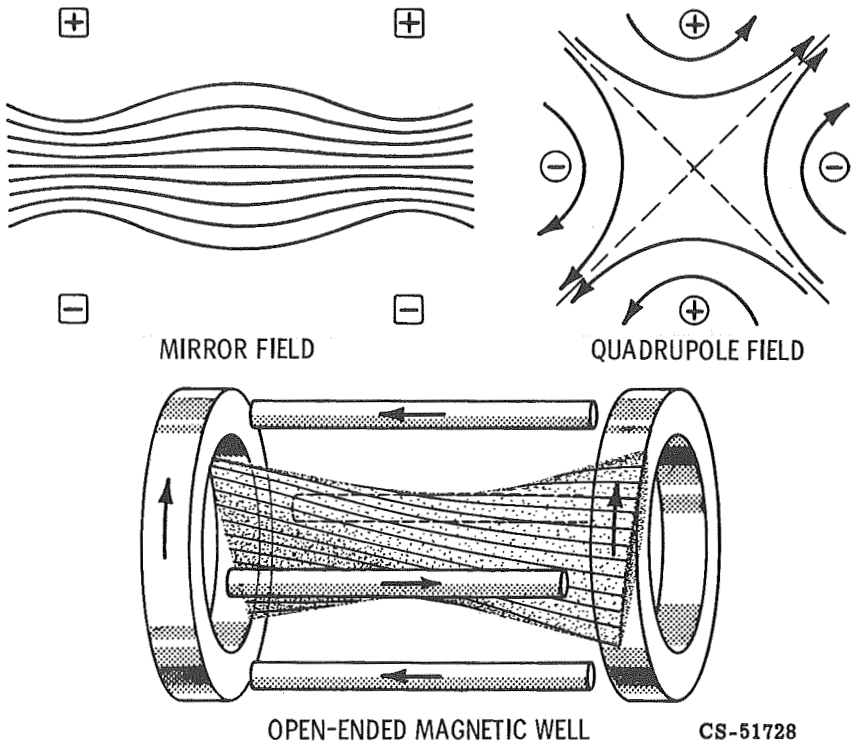

Figure III-4. - Plasma confined in open-ended magnetic well.

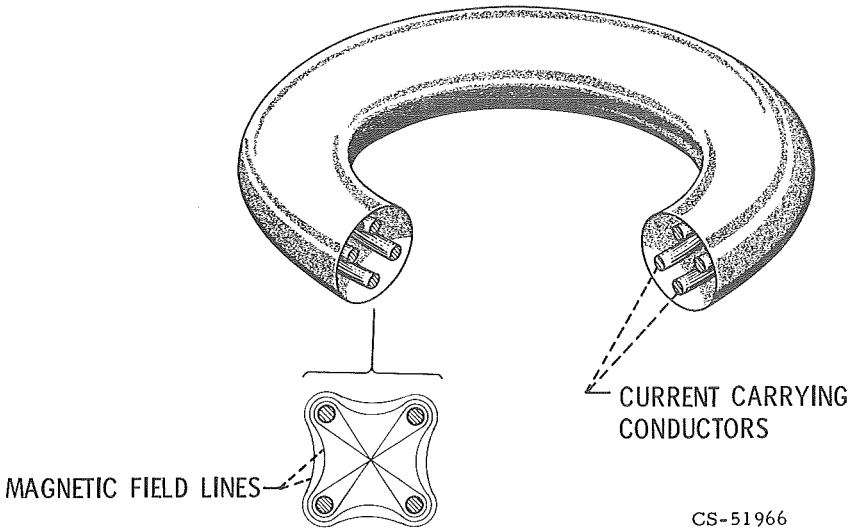

Figure III-5. - Toroidal magnetic-well geometry.

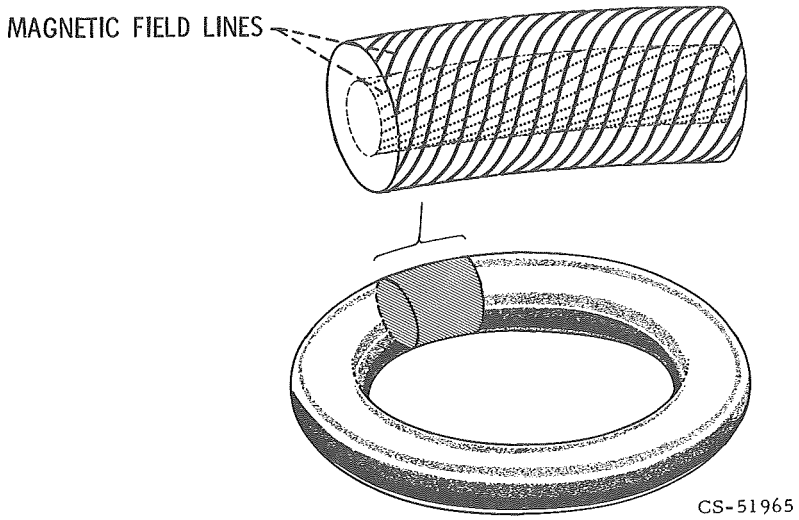

Figure III-6. - Toroidal magnetic field with shear.

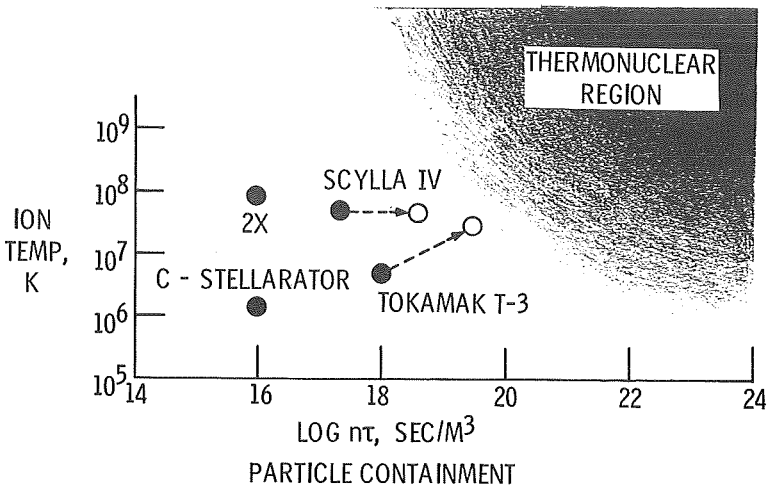

Figure III-7. - Lawson diagram.

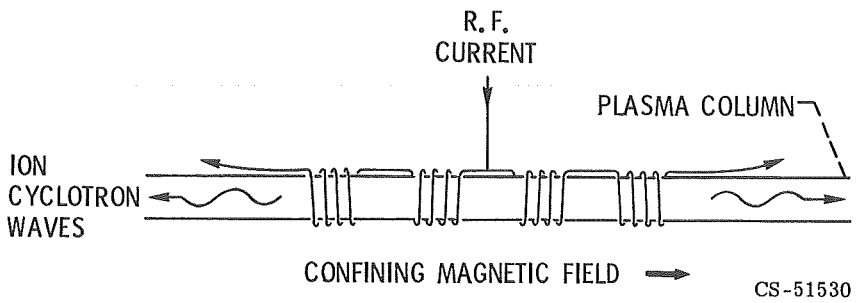

Figure III-8. - Four-section Stix coil for generating ion-cyclotron waves.

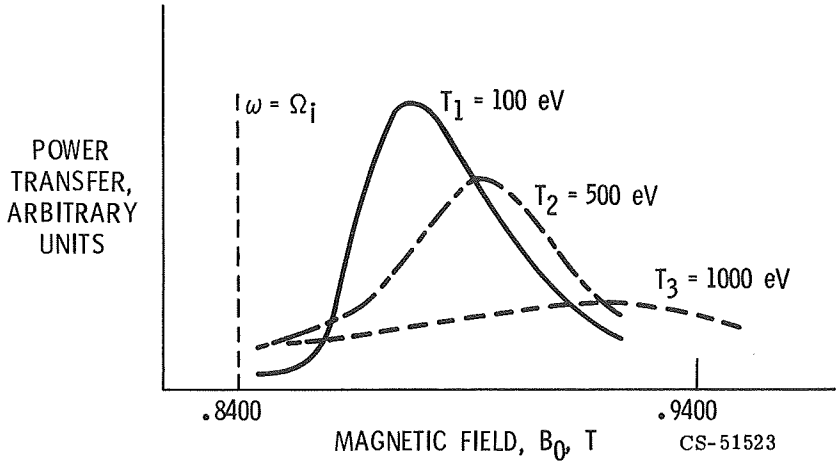

Figure III-9. - Theoretical power transfer as function of magnetic field with ion temperature as parameter.

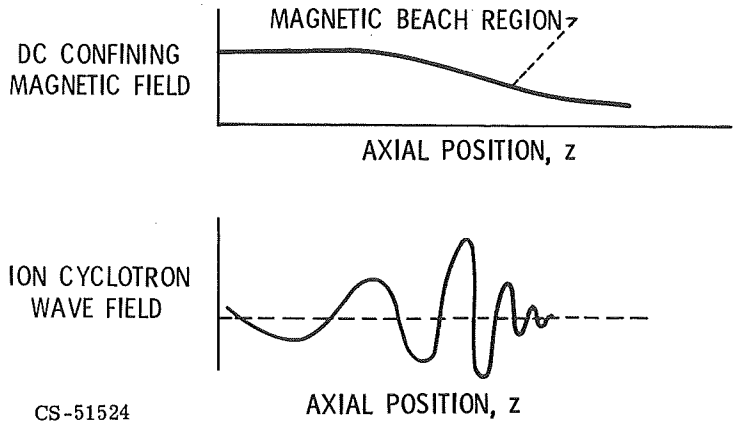

Figure III-10. - Wave damping in magnetic beach.

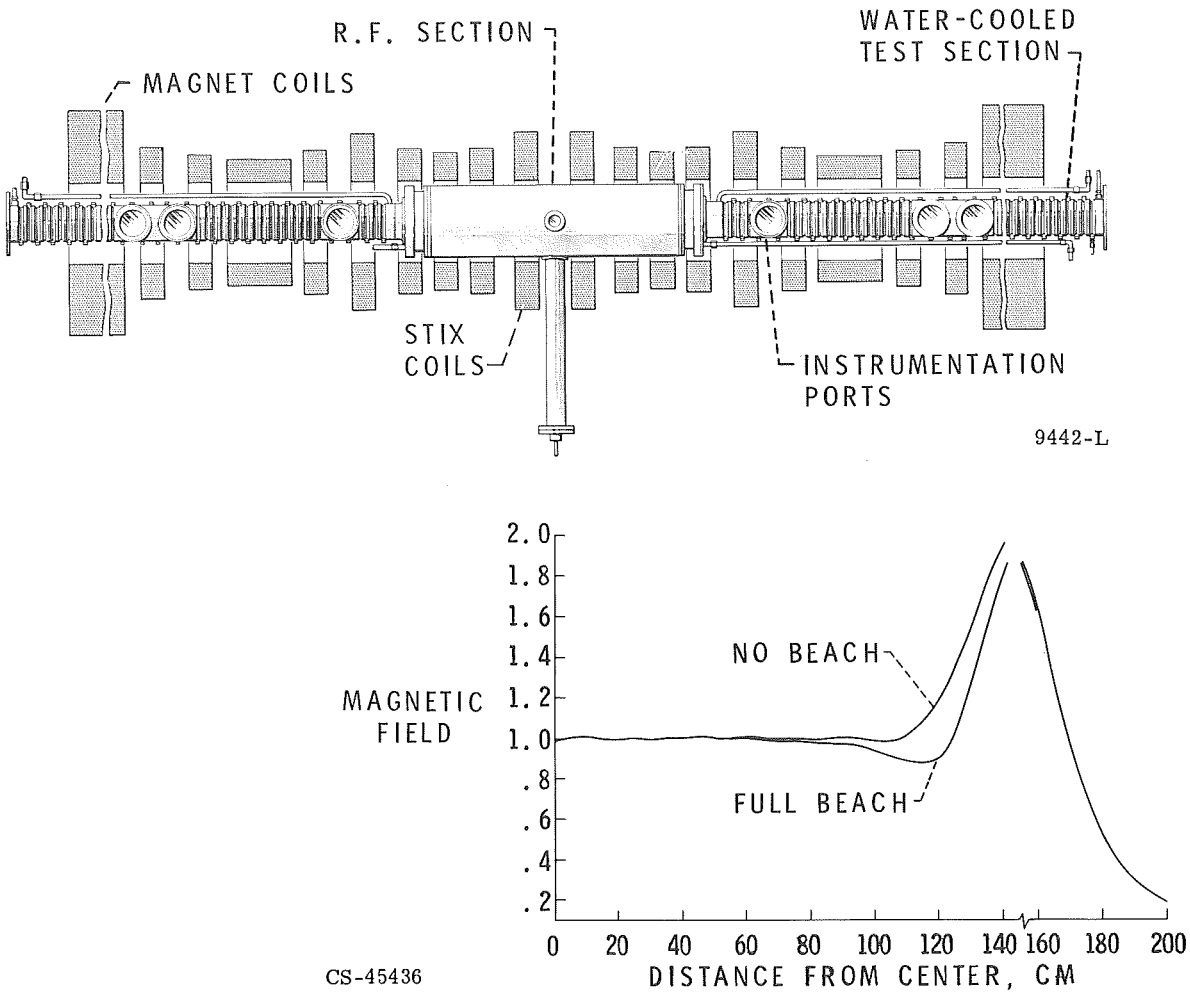

Figure III-11. - Ion cyclotron resonance apparatus.

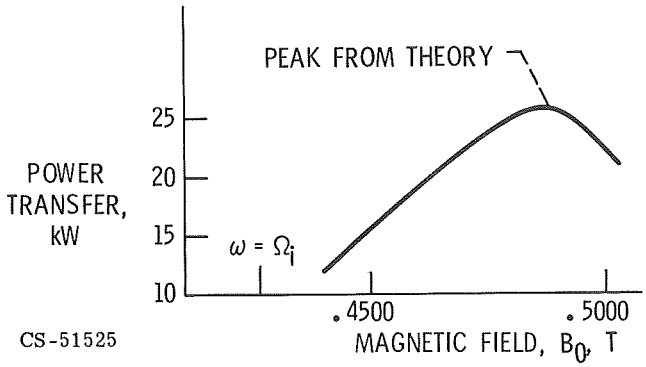

Figure III-12. - Experimental power transfer as function of magnetic field.

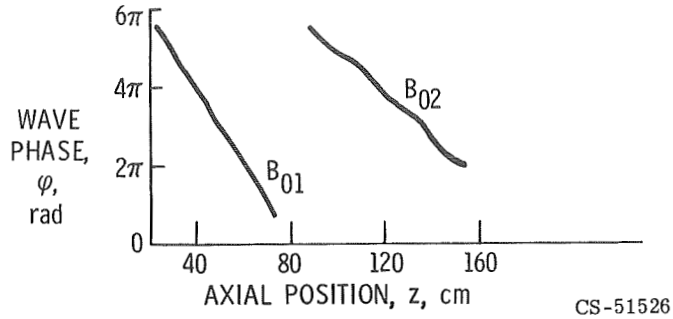

Figure III-13. - Ion-cyclotron wave phase for B_z as function of axial position for two values of magnetic field ($B_{01} < B_{02}$).

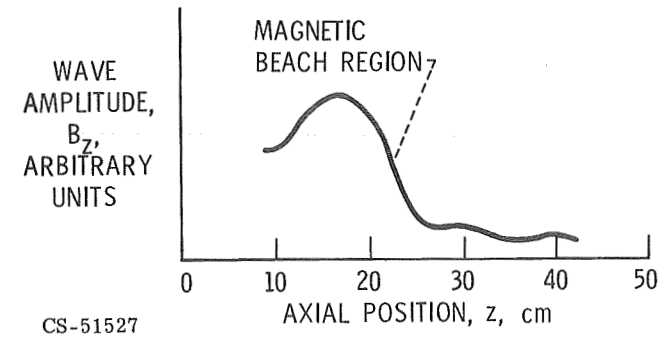

Figure III-14. - Ion-cyclotron wave amplitude B_z as function of axial position.

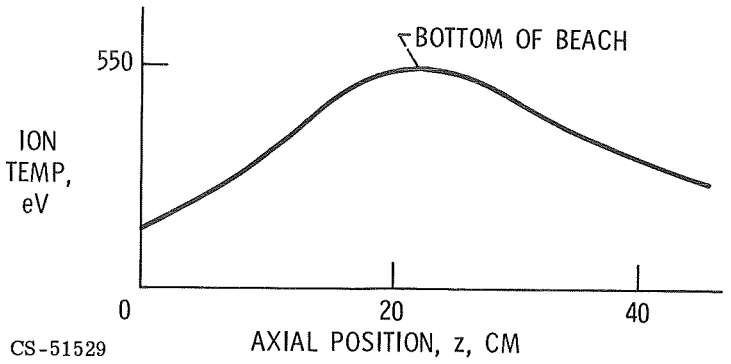

Figure III-15. - Ion temperature from diamagnetic loop in beach region.

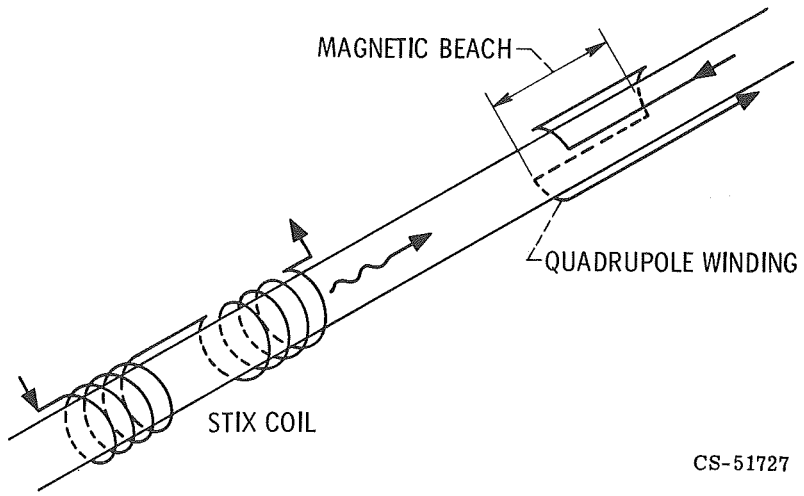

Figure III-16. - Experimental arrangement to study ion-cyclotron wave propagation in magnetic well.

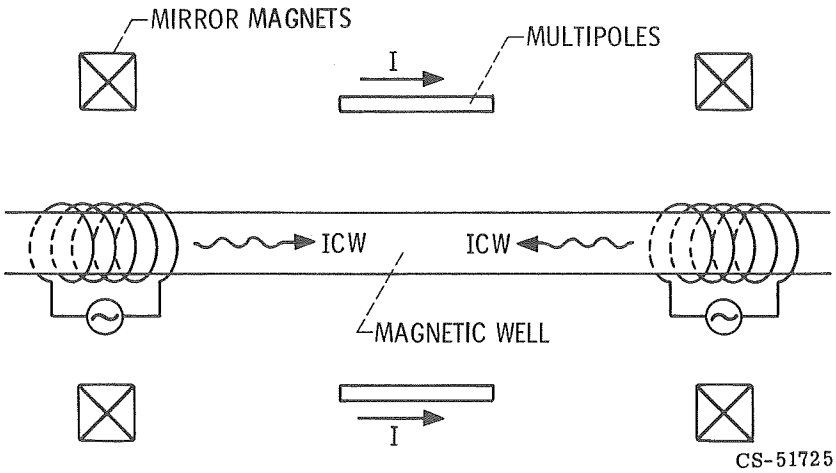

Figure III-17. - Ion cyclotron resonance heating applied to open magnetic wells.

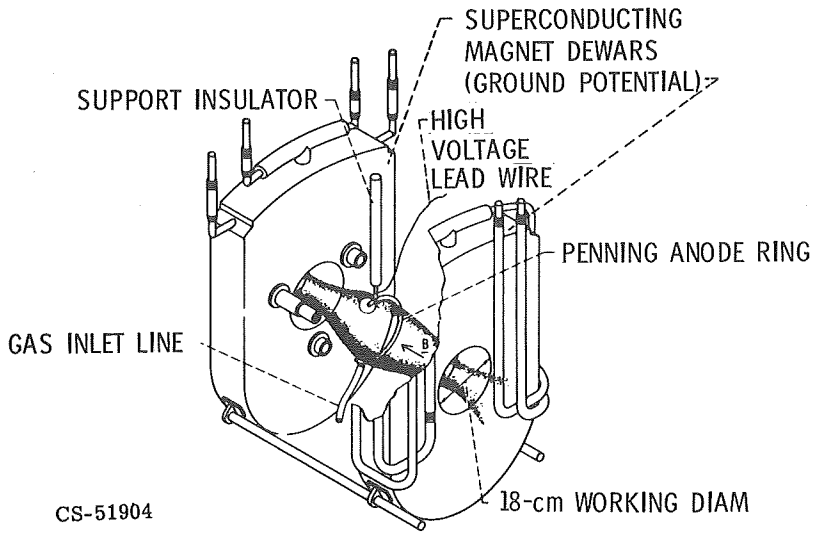

Figure III-18. - Discharge operating configuration and detail of anode ring.

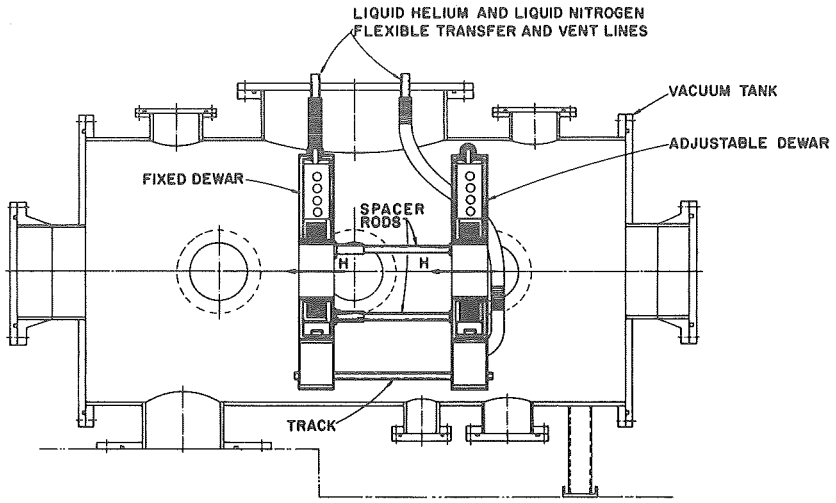

CS-35346

Figure III-19. - Isometric cutaway drawing of vacuum tank.

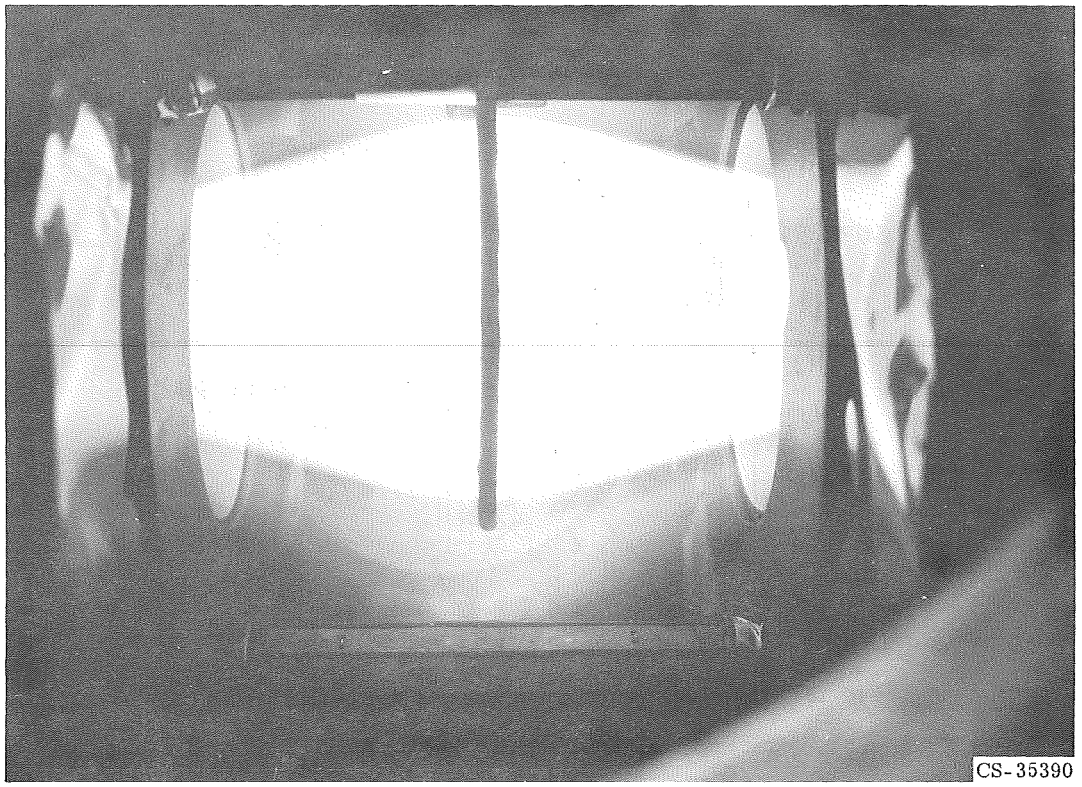

CS-35390

Figure III-20. - Photograph of plasma.

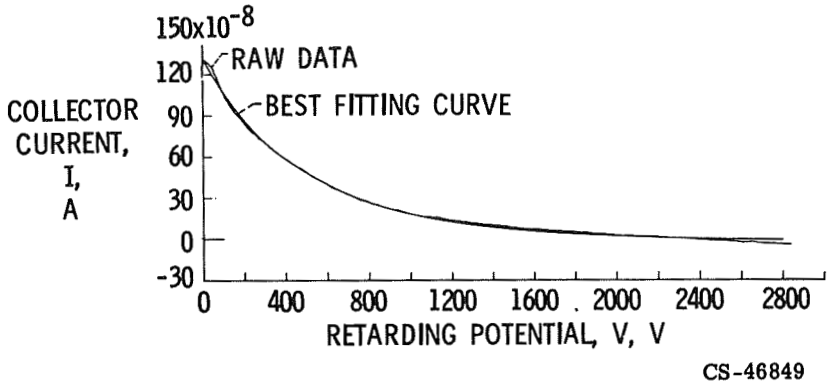

Figure III-21. - Measurement of retarding potential-energy analyzer. Kinetic temperature, 710 electron volts.

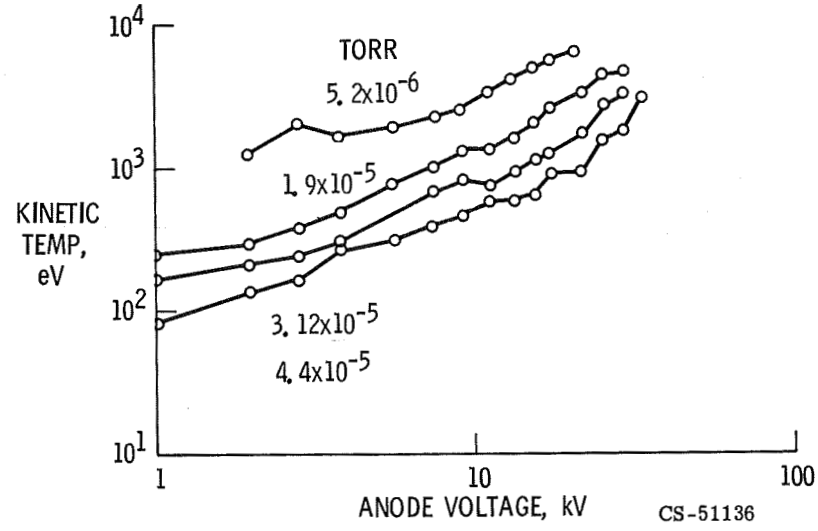

Figure III-22. - Relation of anode voltage to deuterium kinetic temperature for various background gas pressure. B_{max} = 2.0 T.

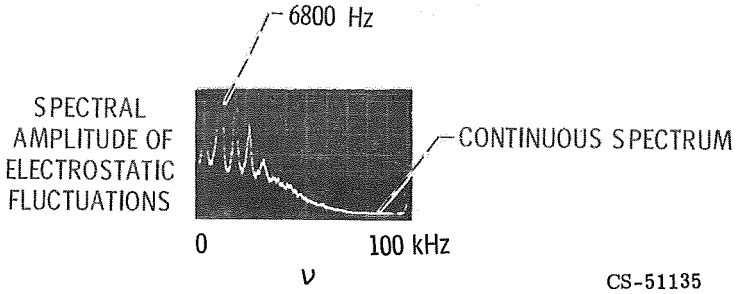

Figure III-23. - Electrostatic potential fluctuations.

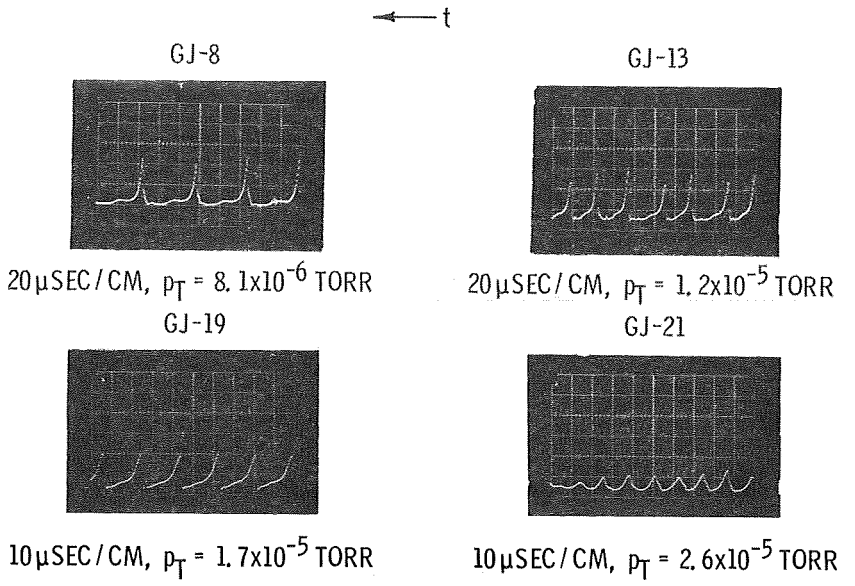

Figure III-24. - Charged particle efflux as function of time.

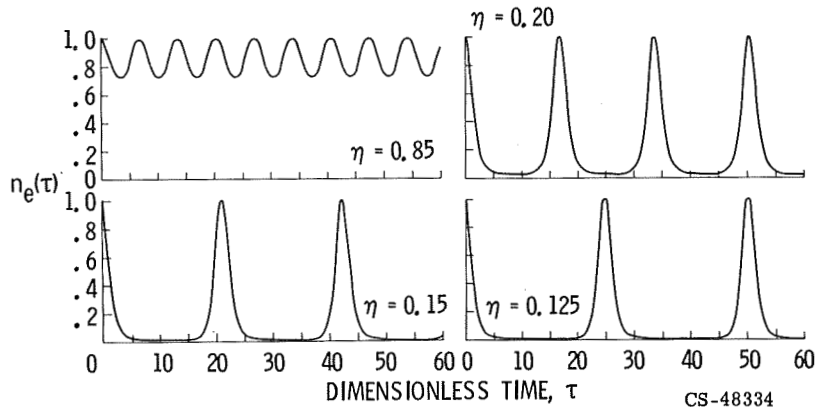

Figure III-25. - Relative number density as function of time.

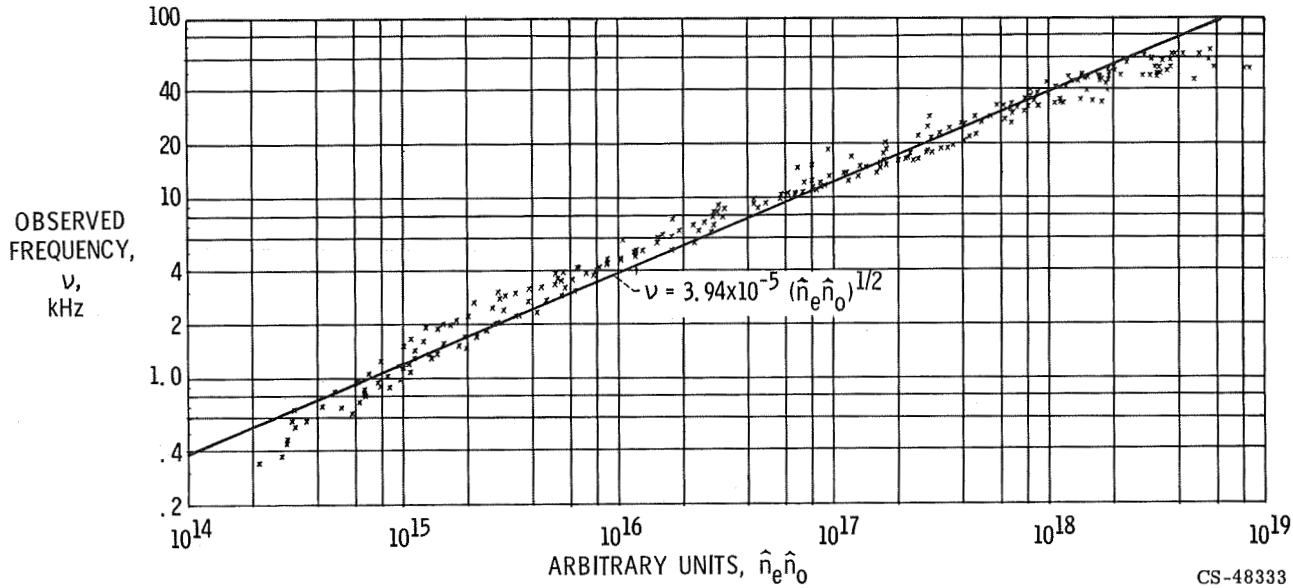

Figure III-26. - Observed frequency as function of product of average electron and neutral number densities.

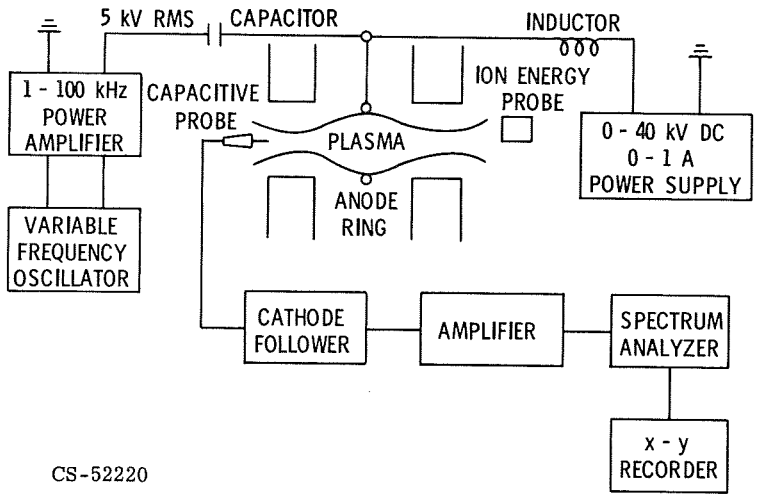

Figure III-27. - Apparatus for investigation of external modulation of anode voltage.

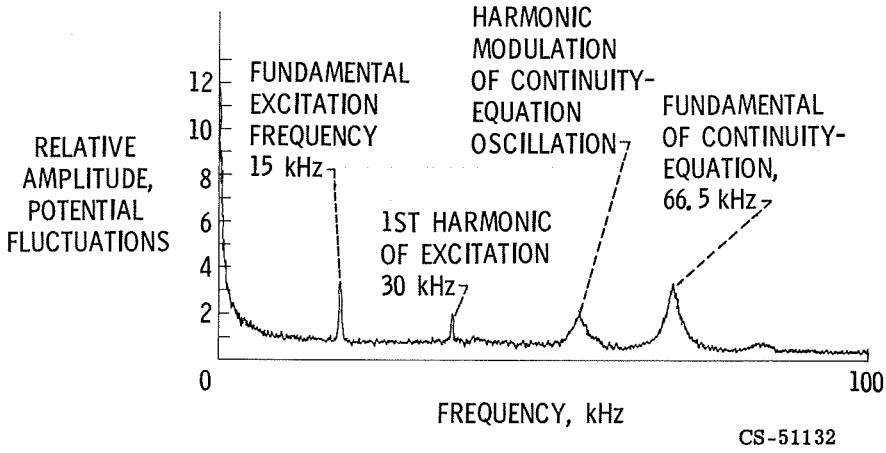

Figure III-28. - Spectrum of potential fluctuations; medium background pressure, 7×10^{-5} torr.

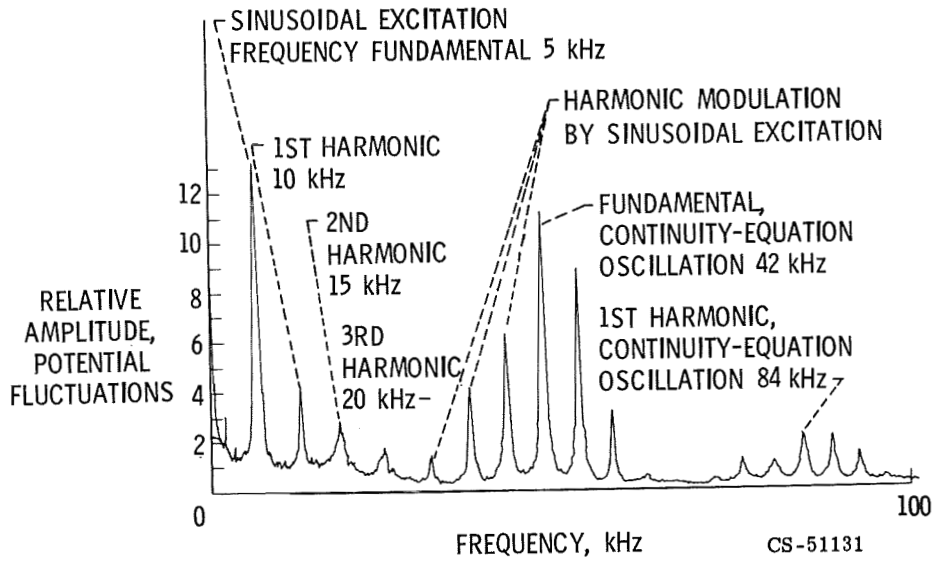

Figure III-29. - Spectrum of potential fluctuations; low background pressure, $\sim 4.5 \times 10^{-5}$ torr.

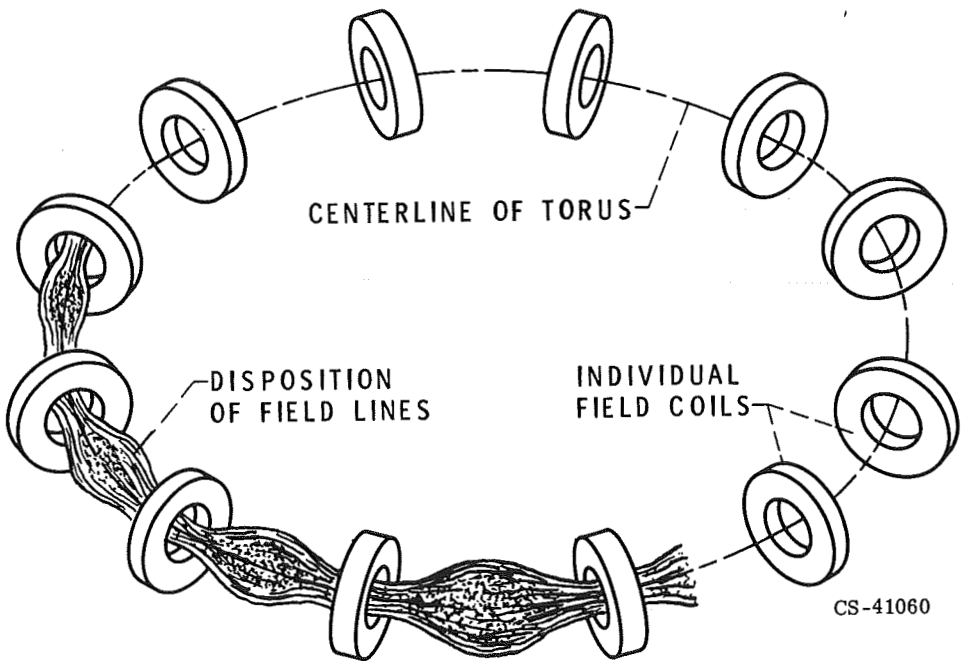

Figure III-30. - Bumpy torus concept.

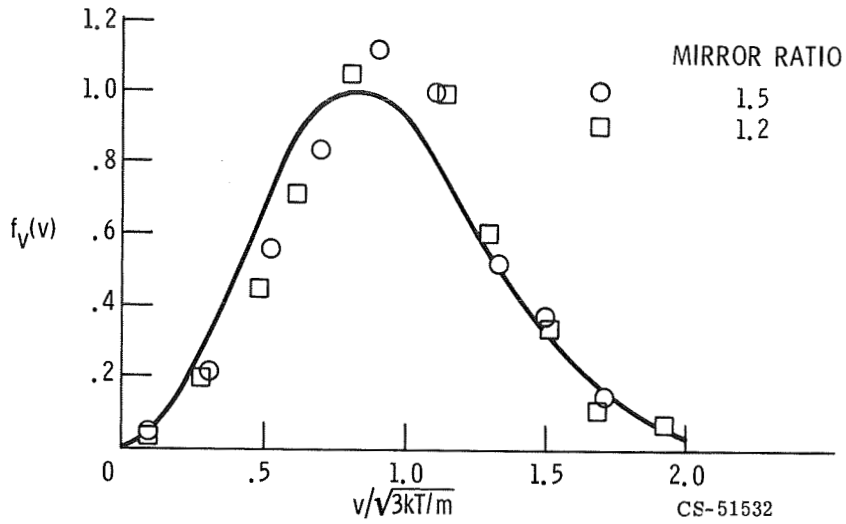

Figure III-31. - Marginal distribution in velocity magnitude.

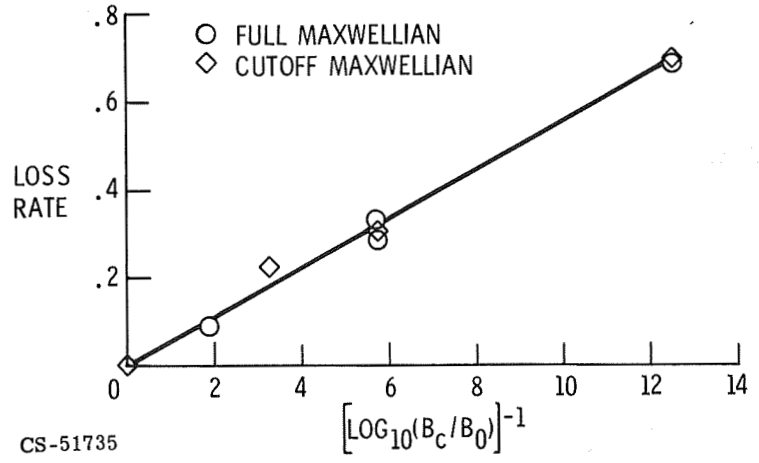

Figure III-32. - Random-walk loss rates.

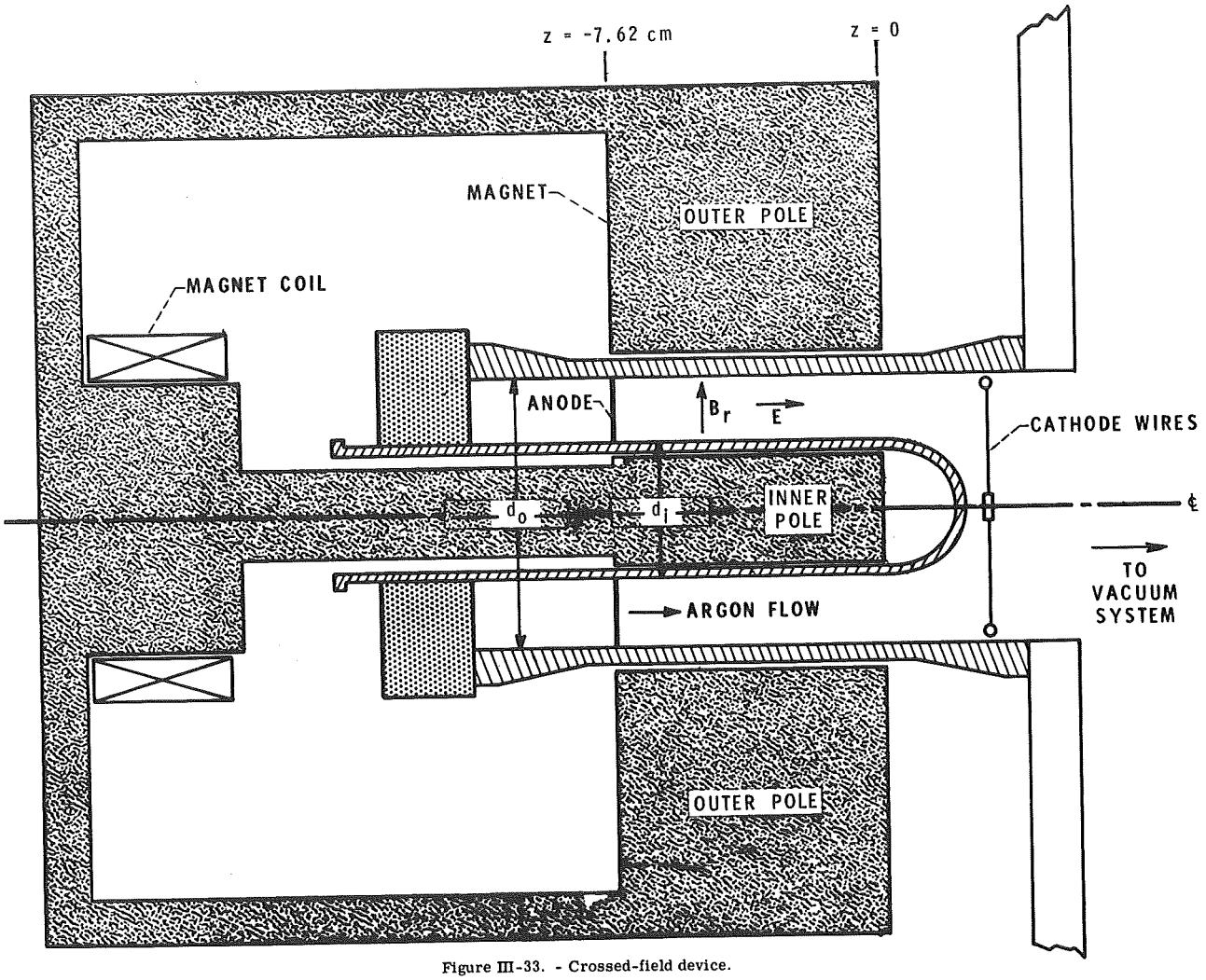

Figure III-33. - Crossed-field device.

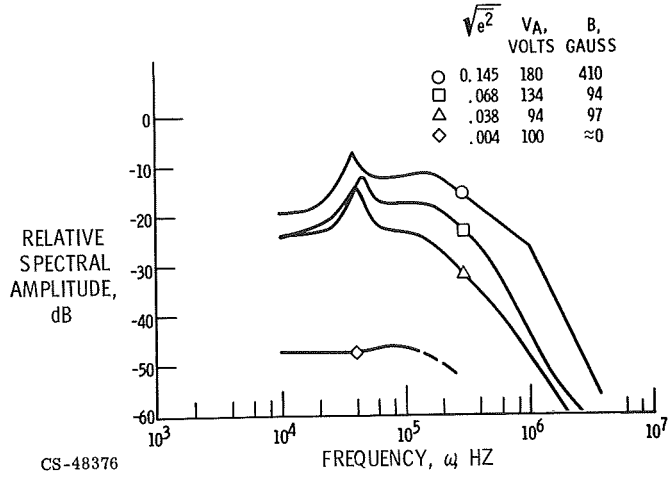

Figure III-34. - Amplitude spectra of plasma fluctuations.